

Reactivity of $\text{Sc}^+(\text{}^3\text{D}, \text{}^1\text{D})$ and $\text{V}^+(\text{}^5\text{D}, \text{}^3\text{F})$: Reaction of Sc^+ and V^+ with Water

Arantxa Irigoras, Joseph E. Fowler, and Jesus M. Ugalde*

Contribution from the Kimika Fakultatea, Euskal Herriko Unibertsitatea, P.K. 1072, 20080 Donostia, Euskadi, Spain

Received February 20, 1998. Revised Manuscript Received August 24, 1998

Abstract: The study of the reaction of water with the early first-row transition metal ions has been completed in this work, in both high- and low-spin states. In agreement with experimental observations, the only exothermic products are the low-lying states $\text{MO}^+ + \text{H}_2$; formation of other endothermic products is also examined. An in-depth analysis of the reaction paths leading to each of the observed products is given, including various minima and several important transition states. All results have been compared with existing experimental data and our earlier work covering the $\text{Ti}^+ + \text{H}_2\text{O}$ reaction in order to observe existent trends for the early first-row transition metal ions.

1. Introduction

The recent excitement in the study of transition metals is in part due to improved methods of studying, both experimentally and theoretically, the plethora of low-lying electronic states and their effects on reaction properties. The different gas-phase reactivity that transition metals show depending on the spin, electron configuration, and even spin-orbit level has been discussed extensively by Armentrout and co-workers.^{1–3} As they have pointed out in those works, studies of excited electronic states of transition metal ions can help validate the molecular orbital ideas that are used routinely to understand the activation of covalent bonds by transition metals. Thus, such studies are a perfect field for interaction between experiment and theory.

The reactions of transition metal cations and water have received much attention recently, in large part due to two curious effects. The first is that the early transition metal cations (Sc^+ , Ti^+ , and V^+) are more reactive than their oxides, while the contrary is true with the late metals (Cr^+ , Mn^+ , and Fe^+).⁴ Even more interesting, however, is that the primary product observed in the reverse reaction ($\text{MO}^+ + \text{H}_2 \rightarrow \text{M}^+ + \text{H}_2\text{O}$) is a low-spin excited state of the cation,⁴ meaning that spin, rather than reaction energetics, is the overriding constraint of the reaction.

With regard to the importance of spin in these reactions, evidence comes from both the forward reaction ($\text{M}^+ + \text{H}_2\text{O} \rightarrow \text{MO}^+ + \text{H}_2$) and its reverse. In the forward transition metal cation plus water reaction, two factors point to the importance of the spin state. The first is that, if ground-state high-spin cations are used for the reaction, the observed MO^+ product is, nevertheless, in its low-spin ground state. Of course, if an excited-state low-spin cation is used, the MO^+ product will also be in its ground state. However, the grand difference between using high-spin or low-spin cations as reactants is not the final product but rather the efficiency of the reaction. While the high-spin cations do react to give low-spin MO^+ products, the

efficiency is actually quite low. On the other hand, the reaction starting with a low-spin cation proceeds rapidly and efficiently.^{5,6}

There is also a point of difference between Sc^+ , Ti^+ , and V^+ that is rather interesting. The ground-state high-spin cations of Sc^+ and Ti^+ do produce (though inefficiently) low-spin MO^+ . However, the ground-state $\text{V}^+(\text{}^5\text{D}(d^4))$ cation *does not* make the spin crossing to produce triplet VO^+ . The first quintet excited state of $\text{V}^+(\text{}^5\text{F}(sd^3))$, on the other hand, follows the trend established by the high-spin Sc^+ and Ti^+ cations, i.e., production of low-spin MO^+ , albeit inefficiently. Of question is whether this is due to the occupation scheme (both high-spin ground-state Sc^+ and Ti^+ have a singly occupied s orbital) or due simply to the extra kick of energy available in the $\text{}^5\text{F}$ state. We address this question in the discussion of the potential energy surfaces.

From the experimental data, we gather that the reaction pathway is a low-spin pathway and that, somewhere along the line, the high-spin complex must undergo a spin-forbidden crossing. The reaction pathway demonstrated in our earlier work is $\text{Ti}^+ + \text{H}_2\text{O} \rightarrow \text{Ti}^+ - \text{OH}_2 \rightarrow \text{HTi}^+\text{OH} \rightarrow (\text{H}_2) - \text{TiO}^+ \rightarrow \text{TiO}^+ + \text{H}_2$. In the $\text{Ti}^+ - \text{OH}_2$ ion-molecule complex, the high-spin state still lies below the low-spin state, but in the HTi^+OH intermediate that situation is reversed, implying that the high- and low-spin surfaces cross between these two moieties.

Another topic of interest concerning these reactions is the process of H_2 elimination (or addition in the reverse reaction). Two possibilities were proposed: elimination from an H_2MO^+ intermediate⁷ or elimination from a four-centered transition state.^{5,6} Our earlier work¹¹ on the high- and low-spin $\text{Ti}^+ + \text{H}_2\text{O}$ reaction does predict a final intermediate before H_2 elimination in which the H atoms are most closely associated with the Ti atom. However, *no* H–Ti covalent σ bonds existed.

(5) Clemmer, D. E.; Chen, Y.-M.; Aristov, N.; Armentrout, P. B. *J. Phys. Chem.* **1994**, *98*, 7538.

(6) Chen, Y. M.; Clemmer, D. E.; Armentrout, P. B. *J. Phys. Chem.* **1994**, *98*, 11490–11498.

(7) Guo, B. C.; Kerns, K. P.; Castleman, A. W. *J. Phys. Chem.* **1992**, *96*, 4879–4883.

(8) Tilson, J. L.; Harrison, J. F. *J. Phys. Chem.* **1991**, *95*, 5097.

(9) Ye, S. *Theochem.* **1997**, *417*, 157–162.

(10) Irigoras, A.; Ugalde, J. M.; Lopez, X.; Sarasola, C. *Can. J. Chem.* **1996**, *74*, 1824–1829.

(11) Irigoras, A.; Fowler, J. E.; Ugalde, J. M. *J. Phys. Chem., A*, **1998**, *102*, 293.

(1) Elkind, J. L.; Armentrout, P. B. *J. Phys. Chem.* **1987**, *91*, 2037–2045.

(2) Armentrout, P. B. *Annu. Rev. Phys. Chem.* **1990**, *41*, 313–344.

(3) Armentrout, P. B. *Science* **1991**, *251*, 175–179.

(4) Clemmer, D. E.; Aristov, N.; Armentrout, P. B. *J. Phys. Chem.* **1993**, *97*, 544–552.

Table 1. Total Energies (*E*), in Hartree, Zero-Point Vibrational Energy Corrections (Δ ZPVE), Basis Set Superposition Error Corrections (BSSE), and Dissociation Energies (*D*₀), in eV, for the M(OH₂)⁺ Ion–Molecule Complexes (M = Sc, Ti, V)

M	method	<i>E</i>	Δ ZPVE	BSSE	<i>D</i> ₀
Sc	B3LYP/DZVP	−836.794 92	0.061	0.056	1.641
	B3LYP/TZVP+G(3df,2p)	−836.916 55	0.065	0.018	1.580
	CCSD(T)/TZVP+G(3df,2p)	−836.187 85	0.065	0.068	1.410
	expt ^{33 a}				1.36 ± 0.13
	theor ³¹				1.497
	theor ⁹				2.500
Ti	B3LYP/DZVP	−925.511 90	0.078	0.039	1.571
	B3LYP/TZVP+G(3df,2p)	−925.649 49	0.074	0.022	1.619
	CCSD(T)/TZVP+G(3df,2p)	−924.877 41	0.074	0.073	1.573
	expt ^{33 a}				1.471
	expt ^{32 b}				1.65 ± 0.13
	theor ³¹				1.60 ± 0.06
V	B3LYP/DZVP	−1020.037 78	0.056	0.039	1.628
	B3LYP/TZVP+G(3df,2p)	−1020.196 40	0.065	0.017	1.588
	CCSD(T)/TZVP+G(3df,2p)	−1019.386 14	0.065	0.065	1.406
	expt ^{33 a}				1.57 ± 0.13
	expt ^{32 b}				1.52 ± 0.05
	expt ^{34 a}				1.523 ± 0.174
	theor ³¹				1.506

^a Temperature not specified. ^b Values at 0 K.

Instead, the intermediate immediately preceding H₂ elimination could be viewed as an ion–molecule complex with some donation of electron density from the H–H σ bond to the Ti atom and some back-donation from a Ti d orbital to the H–H σ^* orbital.

Multiconfiguration self-consistent field (MCSCF) and configuration interaction (MCSCF+1+2) calculations⁸ have been already done for some of the products of the reaction Sc⁺(³D) + H₂O. Also, a MP4(SDTQ)**//MP2/6-31G** study of the dehydrogenation reaction of water by Sc⁺ has recently appeared in the literature.⁹ No previous theoretical works have appeared on the vanadium system. We present the full reaction mechanism geometries and energetics for both the high- and low-spin states, considering the possible transition states.

2. Methods

The experience of this group^{10,11} shows that the density functional theory (B3LYP functional)^{12,13} with the DZVP basis sets given by Salahub et al.^{14,15} is a reasonable choice for optimization and frequency calculations of these systems. Recent calibration calculations on transition metal compounds affirm this choice.¹⁶ The choice of the B3LYP DFT method is largely motivated by its satisfactory performance reported recently¹⁶ for transition-metal-containing systems. Reactants and products of the possible reactions have been reoptimized at the B3LYP/TZVP+G(3df,2p) level of theory. All the calculations have been corrected with the ZPVE calculated at the corresponding theoretical level.

To confirm the B3LYP results, some single-point CCSD(T)/TZVP+G(3df,2p) calculations have been carried out at the B3LYP/TZVP+G(3df,2p) equilibrium geometries. The 1s electrons of O and 1s to 2p electrons of the metals were frozen in the CCSD(T) calculations.

The triple- ζ quality basis set, TZVP+G(3df,2p), used for titanium was that given by Schäfer, Hubert, and Ahlrichs,²³ supplemented with a diffuse s function (with an exponent 0.33 times that of the most diffuse s function on the original set), two sets of p functions optimized by Wachters²⁴ for the excited states, one set of diffuse pure angular momentum d function (optimized by Hay),²⁵ and three sets of uncontracted pure angular momentum f functions, including both tight and diffuse exponents, as recommended by Ragavachari and Trucks.²⁶ For the oxygen and hydrogen atoms, the 6-311++G(2df,2p) basis set of Pople et al.²⁷ was used.

All DFT and CCSD(T) calculations reported in this paper have been carried out with the GAUSSIAN94/DFT²⁸ suites of programs. Also,

NBO^{29,30} calculations have been done to give additional insight into the bonding properties of some structures.

3. Results and Discussion

3.1. Dissociation Energies. Dissociation energies of the Sc(OH₂)⁺ and V(OH₂)⁺ ion–molecules calculated at the B3LYP/DZVP, B3LYP/TZVP+G(3df,2p), and CCSD(T)/P+G(3df,2p) levels of theory are shown in Table 1. Results for the Ti(OH₂)⁺ ion–molecule at the same levels of theory^{10,11} are shown also. Dissociation energies were calculated as the

- (12) Becke, A. D. *Phys. Rev. A* **1988**, *38*, 3098.
 (13) Lee, C.; Yang, W.; Parr, R. G. *Phys. Rev. B* **1988**, *37*, 785.
 (14) Sim, F.; Salahub, D. R.; Chim, S.; Dipuis, M. *J. Chem. Phys.* **1991**, *95*, 4317.
 (15) Godbout, N.; Salahub, D. R.; Andzelm, J.; Wimmer, E. *Can. J. Chem.* **1992**, *70*, 560.
 (16) Bauschlicher, C. W., Jr.; Ricca, A.; Partridge, H.; Langhoff, S. R. *In Recent Advances in Density Functional Theory*; Chong, D. P., Ed.; World Scientific Publishing Co.: Singapore, 1997; Part II.
 (17) Sodupe, M.; Branchadell, V.; Rosi, M.; Bauschlicher, C. W., Jr. *J. Phys. Chem.* **1997**, *101*, 7854–7859.
 (18) Siegbahn, P. E. M. *Electronic structure calculations for molecules containing transition metals*; Advances in Chemical Physics XCIII; Wiley: New York, 1996.
 (19) Ricca, A.; Bauschlicher, C. W. *J. Phys. Chem.* **1994**, *98*, 12899.
 (20) Bauschlicher, C. W.; Maitre, P. *J. Phys. Chem.* **1995**, *99*, 3444.
 (21) Hartmann, M.; Clark, T.; Eldik, R. van. *J. Am. Chem. Soc.* **1997**, *119*, 7843.
 (22) Pavlov, M.; Siegbahn, P. E. M.; Sandström, M. *J. Phys. Chem. A* **1998**, *102*, 219.
 (23) Schäfer, A. Hurbert, C.; Ahlrichs, R. *J. Chem. Phys.* **1994**, *100*, 5829.
 (24) Wachters, A. J. *J. Chem. Phys.* **1970**, *52*, 1033.
 (25) Hay, P. J. *J. Chem. Phys.* **1971**, *66*, 4377.
 (26) Raghavachari, K.; Trucks, G. W. *J. Chem. Phys.* **1989**, *91*, 1062.
 (27) Krishnan, J. S.; Binkley, J. S.; Seeger, P. v. R.; Pople, J. A. *J. Chem. Phys.* **1980**, *72*, 650.
 (28) Frish, M. J.; Trucks, G. W.; Schlegel, H. B.; Gill, P. M. W.; Johnson, B. G.; Robb, M. A.; Cheeseman, J. R.; Keith, T. A.; Petersson, G. A.; Montgomery, J. A.; Raghavachari, K.; Al-Laham, M. A.; Zakrzewski, V. G.; Ortiz, J. V.; Foresman, J. B.; Cioslowski, J.; Stefanov, B. B.; Nanayakkara, A.; Challacombe, M.; Peng, C. Y.; Ayala, P. Y.; Chen, W.; Wong, M. W.; Andres, J. L.; Replogle, E. S.; Gomperts, R.; Martin, R. L.; Fox, D. J.; Binkley, J. S.; Defrees, D. J.; Baker, J.; Stewart, J. P.; Head-Gordon, M.; Gonzalez, C.; Pople, J. A. *Gaussian 94* (Revision A.1); Gaussian, Inc.: Pittsburgh, PA, 1995.
 (29) Read, A. E.; Curtiss, L. A.; Weinhold, F. *Chem. Rev.* **1988**, *88*, 899.
 (30) Glendening, A. E.; Read, A. E.; Carpenter, J. E.; Weinhold, F. *NBO*, Version 3.1.

Table 2. Relative Energies, in eV, for the $^3\text{D}(\text{sd})$ and Closed-Shell Singlet $^1\text{D}(\text{s}^2)$ State of Sc^+ (Δ_1), the $^3\text{D}(\text{sd})$ and Open-Shell Singlet $^1\text{D}(\text{sd})$ States of $\text{Sc}^+(\Delta_2)$, the $^3\text{A}_2$ and Closed-Shell Singlet $^1\text{A}_1$ States of $\text{Sc}(\text{OH}_2)^+$ (Δ_3), the $^3\text{A}_2$ and Open-Shell Singlet $^1\text{A}_1$ States of $\text{Sc}(\text{OH}_2)^+$ (Δ_4), and the $^3\Delta$ and $^1\Sigma$ States of ScO^+ (Δ_5)

method	D1	D2	D3	D4	D5
B3LYP/DZVP	0.891	0.169	0.713	0.180	-3.081
B3LYP/TZVP+G(3df,2p)	0.916	0.173	0.697	0.211	-3.192
CCSD(T)/TZVP+G(3df,2p)	0.550	0.154	0.375	0.225	-3.496
expt ^{6,35}	0.32				
theor ⁸					3.45
theor ⁹	0.304	0.543		5.234 ^a	

^a This energy difference corresponds to the $^3\Sigma$ and $^1\Sigma$ states.

Table 3. Relative Energies, in eV, for the $^5\text{D}(\text{d}^4)$ and $^3\text{F}(\text{sd}^3)$ States of $\text{V}^+(\Delta_1)$, the $^5\text{A}_1$ and $^3\text{A}_1$ States of $\text{V}(\text{OH}_2)^+$ (Δ_2), and the $^5\Sigma$ and $^3\Sigma$ States of VO^+ (Δ_3)

method	Δ_1	Δ_2	Δ_3
B3LYP/DZVP	0.965	0.889	-2.654
B3LYP/TZVP+G(3df,2p)	0.923	0.783	-2.677
CCSD(T)/TZVP+G(3df,2p)	0.860	0.660	-2.920
expt ^{6,35}	1.07	0.6 ^a	
expt ³⁶	3.3-4.2		

^a Estimated.

difference between the energy of the isolated monomers and the complex, including both BSSE and ZPVE corrections. $\text{M}(\text{OH}_2)^+$ dissociation energies predicted by various levels of theory³¹ and those experimentally observed³²⁻³⁴ are given also in Table 1. Note that the temperature of the works in refs 33 and 34 is not specified.

Good values are obtained with both the B3LYP and CCSD(T) methods when used in conjunction with the TZVP+G-(3df,2p) basis set, as was expected from our experience with the Ti calculations. The difference found between the B3LYP/DZVP and B3LYP/TZVP+G(3df,2p) results is around 0.050 eV, and both are in reasonable agreement with the experimental and theoretical values that can be found in Table 1, especially the more recent and precise data from Armentrout's group. The CCSD(T) values are systematically lower, as is usual for dissociation energies. Test works with the DZVP basis set have shown that the use of a larger basis set is essential with the CCSD(T) method, as CCSD(T)/DZVP dissociation energies were drastically smaller. The MP4(SDTQ)**//MP2/6-31G** values⁹ are clearly too large, implying that this is not a good method for treating this system, as has been proven by other authors.¹⁹

3.2. Excitation Energy. In the reactions of interest, there are three high-low-spin relative energies that are exceptionally important; thus, we describe them more exhaustively. These three are the M^+ , $\text{M}(\text{OH}_2)^+$, and MO^+ moieties. Excitation energies for these systems are shown in Tables 2 ($\text{M} = \text{Sc}$) and 3 ($\text{M} = \text{V}$).

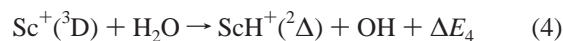
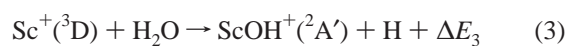
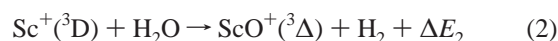
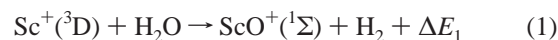
There are two values for single-triplet splittings of both Sc^+ and $\text{Sc}(\text{OH}_2)^+$ given in Table 1. Considering first the cationic atom, the larger of the two splittings is the separation between the triplet and the closed-shell singlet, and the result in relative agreement with the experimental value (though slightly underestimated) is the separation between the triplet and the open-shell singlet. The V^+ singlet-triplet splittings are also lower

than the experimental values given by Moore.³⁵ However, the ordering of the states is correct, and the relative gaps are reasonably well described, and these are the important points for a correct understanding of the PESs.

High-low-spin excitation energies for the $\text{M}(\text{OH}_2)^+$ ion-molecules also have been calculated. The experimental values for these excitation energies are estimations. Thus we compare the theoretical values. In the case of the $^3\text{A}_2 \rightarrow$ (closed-shell) $^1\text{A}_1$ excitation of $\text{Sc}(\text{OH}_2)^+$, the B3LYP and CCSD(T) predictions using the large basis set lie to either side of the values predicted by Ye.⁹ The predictions for the triplet \rightarrow open-shell singlet excitation energy show less variance and are slightly greater than those of the Sc^+ cation. For the vanadium system, the disagreement between the B3LYP and CCSD(T) is less than was seen for the open- to closed-shell excitation of the $\text{Sc}(\text{OH}_2)^+$ complex, and the agreement with the experimental estimation is reasonable.

The last system studied at these levels was the MO^+ molecule. Here, the low-spin moieties are the ground states, as was expected, and open-shell low-spin cases need not be considered. Our values agree much better with the estimated experimental values than do Ye's values for ScO^+ . Also, we note that the CCSD(T) numbers are closer to the experimental values than are the B3LYP numbers.

3.3. Reaction Energetics. 3.3.1. $\text{Sc}^+(^3\text{D},^1\text{D}) + \text{H}_2\text{O}$.



Equations 1-4 represent the main ionic products observed in the reaction of $\text{Sc}^+(^3\text{D},^1\text{D})$ with H_2O . The various predicted values and the energies given by Armentrout and co-workers⁶ experimentally, and Tilson and co-workers⁸ and Ye⁹ theoretically, are listed in Table 4.

In agreement with experiment, we find only one definitely exothermic reaction, the formation of low-spin $\text{ScO}^+ + \text{H}_2$ (reaction 1). Our best value of 1.956 eV is in good agreement with the experimental values listed in Table 4, and even our worst value obtained with the B3LYP/DZVP level of theory, 1.689 eV, is better than the value given by Tilson. Again, it is seen that the Moller-Pleset methods give poor values, 4.687 eV in this case. The energies shown for reaction 2 reflect the already discussed $^3\Delta \rightarrow ^1\Sigma\text{ScO}^+$ excitation energy.

Our results also indicate that the reaction leading to $\text{ScOH}^+(^2\text{A}') + \text{H}$ (reaction 3) would be exothermic, but only very slightly so. The experimental result⁶ is that this reaction would be very slightly endothermic. While our numbers are on the opposite side of zero from the experimental numbers, the error is still quite small.

The agreement between our results and the experimental value for reaction 4 is also quite good. Thus, we see that, for each of

(35) Moore, C. E. *Atomic Energy Levels*; NBS Circular 1959; National Bureau of Standards: Washington, DC, 1952; Vol. 2, 3, p 467.

(36) Dyke, J. M.; Gravenor, B. W. J.; Hastings, M. P.; Morris, A. J. *Phys. Chem.* **1985**, 89, 4613.

(37) *CRC Handbook of Chemistry and Physics*, 63rd ed.; Weast, R. C., Ed.; CRC Press: Boca Raton, FL, 1982.

(38) Murad, E. J. *J. Geophys. Res.* **1978**, 83, 5525.

(39) Kang, H.; Beauchamp, J. L. *J. Am. Chem. Soc.* **1986**, 108, 5663.

(40) Aristov, N.; Armentrout, P. B. *J. Am. Chem. Soc.* **1984**, 106, 4065.

(31) Rosi, M.; Bauschlicher, C. W. *J. Chem. Phys.* **1989**, 90 (12), 7264.

(32) Dalleska, N. F.; Honma, K.; Sunderlin, L. S.; Armentrout, P. B. *J. Am. Chem. Soc.* **1994**, 116, 3519.

(33) Magnera, T. F.; David, D. E.; Michl, J. *J. Am. Chem. Soc.* **1989**, 111, 4100.

(34) Marinelli, P. J.; Squires, R. R. *J. Am. Chem. Soc.* **1989**, 111, 4101.

Table 4. Overall Energies for Reactions 1–4 at Several Levels of Theory^a

method	ΔE_1	ΔE_2	ΔE_3	ΔE_4
B3LYP/DZVP	1.689	-1.392	0.084	-2.429
B3LYP/TZVP+G(3df,2p)	1.939	-1.253	0.180	-2.401
CCSD(T)/TZVP+G(3df,2p)	1.956	-1.518	0.010	-2.665
expt ⁶	2.03 ± 0.06		-0.04 ± 0.009	-2.74 ± 0.09
expt ^{37–40}	1.866 ± 0.304			
theor ⁸	1.415	-2.035	-0.395	
theor ⁹	4.687	-0.547 ^b		

^a Energies given are in eV and for the various B3LYP levels of theory include ZPVE corrections calculated at the corresponding level of theory.

^b This energy difference corresponds to the ³Σ and ¹Σ states.

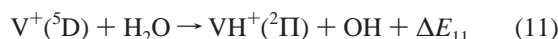
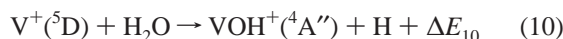
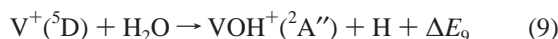
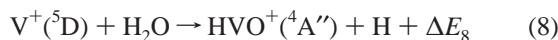
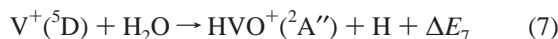
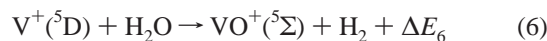
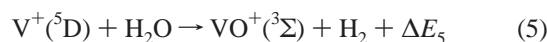
Table 5. Overall Energies for Reactions 5–12 at Several Levels of Theory^a

method	ΔE_5	ΔE_6	ΔE_7	ΔE_8	ΔE_9	ΔE_{10}	ΔE_{11}	ΔE_{12}
B3LYP/DZVP	0.569	-2.085	-2.560	-3.769	-1.687	-0.878	-4.548	-2.854
B3LYP/TZVP+G(3df,2p)	0.687	-1.990	-2.229	-3.559	-1.540	-0.780	-4.499	-2.767
CCSD(T)/TZVP+G(3df,2p)	0.726	-2.169	-2.234	-3.434	-1.608	-0.855	-4.736	-2.945
expt ⁵	0.88 ± 0.10					-0.71 ± 0.15		-3.12 ± 0.06

^a Energies given are in eV and for the various B3LYP levels of theory include ZPVE corrections calculated at the corresponding level of theory.

these reactions, our results hold well with the experiments. It should be noted that the CCSD(T)/TZVP+G(3df,2p) results calculated at the B3LYP/TZVP+G(3df,2p) geometries are especially satisfying.

3.3.2. V⁺(⁵D, ³F) + H₂O.



Equations 5–12 represent the main ionic products observed in the reaction of V⁺(⁵D, ³F) and H₂O. The various predicted values and the energies given by Armentrout and co-workers⁵ are listed in Table 5. No other theoretical values have been published for this system, as far as we know.

Our theoretical estimations for the only exothermic reaction, which leads to VO⁺(³Σ) + H₂, are again below the value given by Armentrout and co-workers, as was also observed for the Sc and Ti cases.

The other experimental results available are those for reactions 10 and 12. For the low-lying endothermic reaction leading to VOH⁺ + H (reaction 10), both the B3LYP and CCSD(T) methods give values within the experimental errors bars when the triple-ζ basis set is used. The predicted values for reaction 12 are slightly lower than the experimental value, but not far off the mark.

3.4. Stationary Points. The following figures show the most relevant stationary points found for the M(OH₂)⁺, TS1⁺, HM⁺OH, TS2⁺, and (H₂)MO⁺ moieties respectively at the B3LYP/DZVP level of theory, where M = Sc, V.

Figure 1 illustrates the M(OH₂)⁺ ion–molecule complexes. The C_{2v} symmetry Sc(OH₂)⁺ ion–molecule complex has a

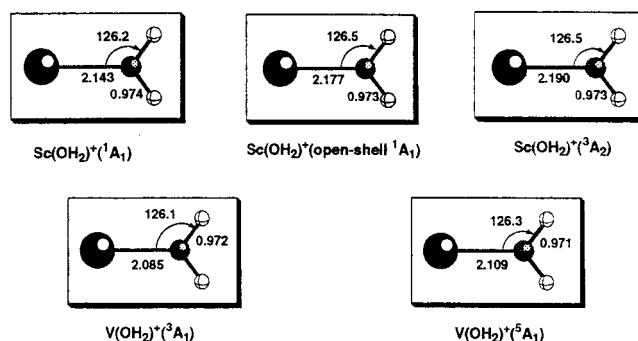


Figure 1. Geometrical parameters of the various M(OH₂)⁺ stationary points on the B3LYP/DZVP potential energy surfaces. Bond lengths are reported in angstroms bond angles in degrees.

Sc–O distance of 2.143 Å in the closed-shell singlet, 2.177 Å in the open-shell singlet, and 2.190 Å in the triplet isomer. The open-shell singlet is closer in geometry (and energy) to the triplet, having similar orbital occupancies. The ground-state open-shell singlet is a ¹A₁ state, but a ¹A₂ state lies very nearby in energy. Similarly, there exists a ³A₁ state lying very near to the ³A₂ ground state.

The V(OH₂)⁺ ion–molecule complex has a V–O distance of 2.085 Å in the low-spin (triplet) case and a bond length of 2.109 Å in the high-spin (quintet) state. The Ti–O bond length in the related doublet and quartet isomers is 2.10 Å.¹¹ Thus, as we progress from Sc to V, this M–O distance shrinks. In all cases, the H₂O moiety itself is only slightly changed from its unassociated parameters, and there is not appreciable difference between the various O–H or M–O–H values.

TS1 shown in Figure 2 characterizes the first hydrogen transfer from oxygen to the metal. This transition state has near-C_s symmetry, and the one imaginary frequency clearly corresponds to hydrogen transfer. Although the exact position of the hydrogen being transferred varies significantly (the surfaces are very flat in this area), again a M–O bond distance decrease is observed from Sc to V.

The HM⁺OH minimum has C_s symmetry. This intermediate is a well-characterized minimum in all reactions. However, there is a large difference between the low- and high-spin M–H bond distances, as can be seen in Figure 3. The low-spin cases follow the expected trend: the M–H bond distance decreases, as does the M–O distance from Sc to V.

The high-spin cases, however, have very long M–H bonds (e.g., 2.606 Å in the HSc⁺OH ³A' isomer). These bonds cannot

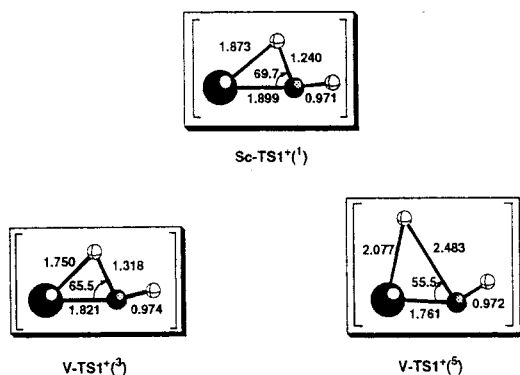


Figure 2. Geometrical parameters of the various TS1⁺ transition states on the B3LYP/DZVP potential energy surfaces. Bond lengths are reported in angstroms, bond angles in degrees.

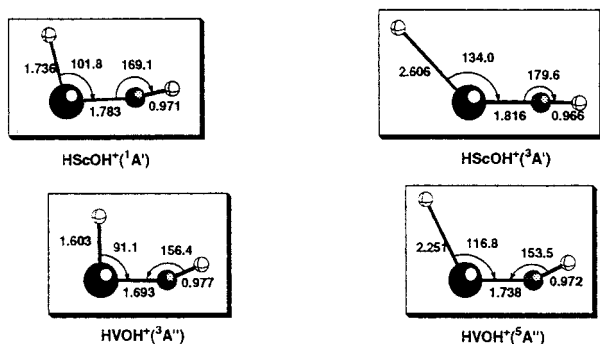


Figure 3. Geometrical parameters of the various HM⁺OH stationary points on the B3LYP/DZVP potential energy surfaces. Bond lengths are reported in angstroms, bond angles in degrees.

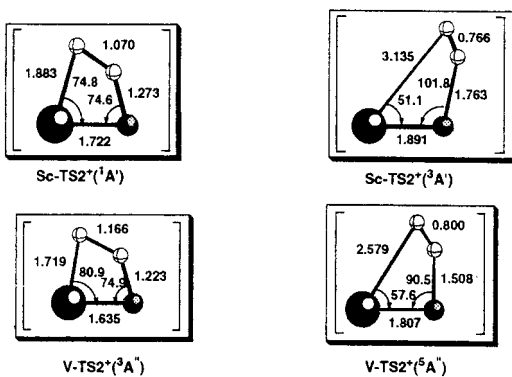


Figure 4. Geometrical parameters of the various TS2⁺ transition states on the B3LYP/DZVP potential energy surfaces. Bond lengths are reported in angstroms, bond angles in degrees.

be considered covalent bonds, and clearly the surfaces are very flat with regard to the movement of this hydrogen, resulting in the large differences seen among the high-spin isomers. We should point out that the M–H distance in HSc⁺OH is remarkably longer than that for the other two cations, as could be expected since no electron is free to contribute to Sc–H bonding. This minimum corresponds essentially to H + ScOH⁺. The Sc–O–H angle also differs from Sc. In this case, we found an angle of almost 180.0°, while for Ti a 160.3° angle was found, and a 153.5° angle was found for V.

The second oxygen-to-scandium hydrogen transfer occurs through TS2 depicted in Figure 4. In the case of the low-spin isomers, these transition states show H–H distances which are still quite long (1.070 Å for Sc, 1.143 Å for Ti,¹¹ and 1.166 Å for V), and the M–O distance (1.722 Å for Sc, 1.666 Å for Ti,¹¹ and 1.635 Å for V) is closer to the HM⁺OH value than

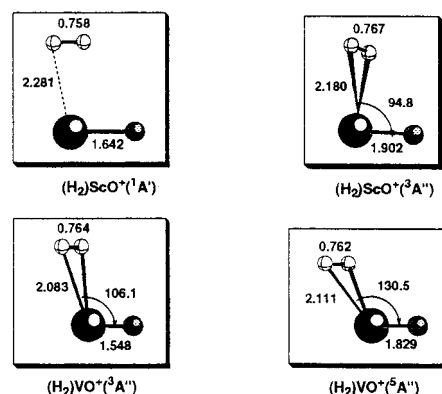


Figure 5. Geometrical parameters of the various (H₂)MO⁺ stationary points on the B3LYP/DZVP potential energy surfaces. Bond lengths are reported in angstroms, bond angles in degrees.

that in the following (H₂)MO⁺ species. The one imaginary frequency corresponds to H–H bond formation and O–H bond-breaking. The high-spin four-centered transition states show an almost-fully formed H–H bond and very long M–H and O–H bond distances. Also, the imaginary frequency is reminiscent of direct H₂ elimination.

The final stationary points located were the (H₂)MO⁺ species illustrated in Figure 5. These (H₂)MO⁺ structures of C_s symmetry are curious intermediates. As it was pointed out for the Ti system,¹¹ this minimum should be considered an ion–molecule complex. Note that the V–H bond distance has incremented from 1.603 Å in the HV⁺OH minimum to 2.083 Å in the corresponding (H₂)VO⁺ minimum. Also the V system, the examination of the MOs shows an interaction between the singly occupied d orbital of M and the σ_{H–H} orbital (see Figure 2 in ref 11). NBO analysis gives this interaction a value of 5.45 kcal/mol for V, smaller than that for the Ti case (7.87 kcal/mol). It is through this interaction that the H–H bond is activated. In comparison with separated low-spin MO⁺ + H₂, the M–O bond length of this complex is only 0.003 Å longer, while the aforementioned H–H bond activation lengthens the H₂ bond length by 0.021 Å. The donation from the σ_{H–H} orbital to the metal s orbital should also be remarked upon, as the NBO analysis gives that donation a value of 7.09 kcal/mol in the case of Ti and 4.87 kcal/mol in the case of V.

In the Sc system, a similar (H₂)ScO⁺ isomer with the hydrogens above and below the plane of symmetry corresponds to a transition state, where the negative eigenvalue corresponds to the rotation of H₂. The local minimum which is found in this region of the singlet PES is a planar (H₂)ScO⁺ structure with a Sc–O bond length only 0.006 Å larger than in the separated ScO⁺ + H₂ products and a H–H distance shorter than that in the other (H₂)MO⁺ structures. Of course, in the singlet (H₂)ScO⁺ system there is no singly occupied d orbital, and thus the d→σ_{H–H} interaction is impossible. Instead, this structure is a dipole-induced ion complex, which clearly would not be possible were the hydrogens located above and below the plane of symmetry. In the NBO analysis of this stationary point, a donation from the σ_{H–H} orbital to the Sc atom was given a value of 9.11 kcal/mol and a donation from the highest σ_{Sc–O} orbital to the σ_{H–H} orbital a value of 4.57 kcal/mol. The triplet (H₂)–ScO⁺ species does have a singly occupied d orbital and follows nicely in the trend set by the other metals.

3.5. Potential Energy Surfaces. Figures 6 and 7 show the potential energy surface starting from the M⁺ + OH₂ separated reactants and leading to MO⁺ + H₂ for the low- and high-spin

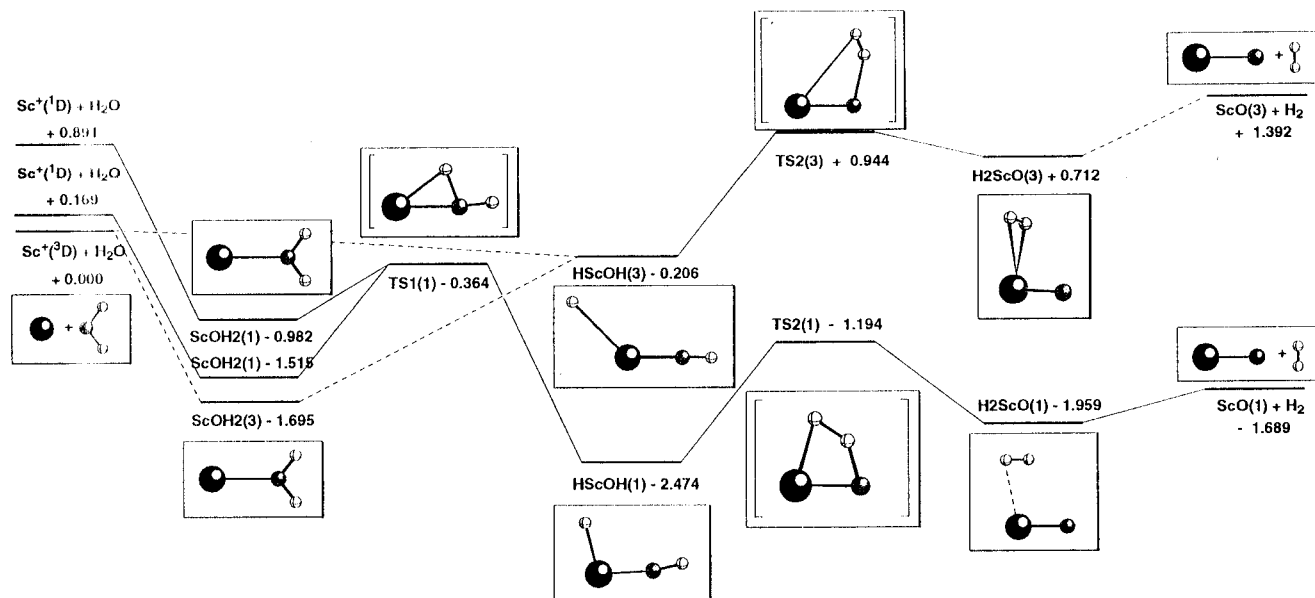


Figure 6. B3LYP/DZVP potential energy surface following the $\text{Sc}^+ + \text{OH}_2 \rightarrow \text{ScO}^+ + \text{H}_2$ reaction path. Energies given are in electronvolts and are relative to the separated ground-state reactants, $\text{Sc}^+(\text{3D}) + \text{OH}_2$.

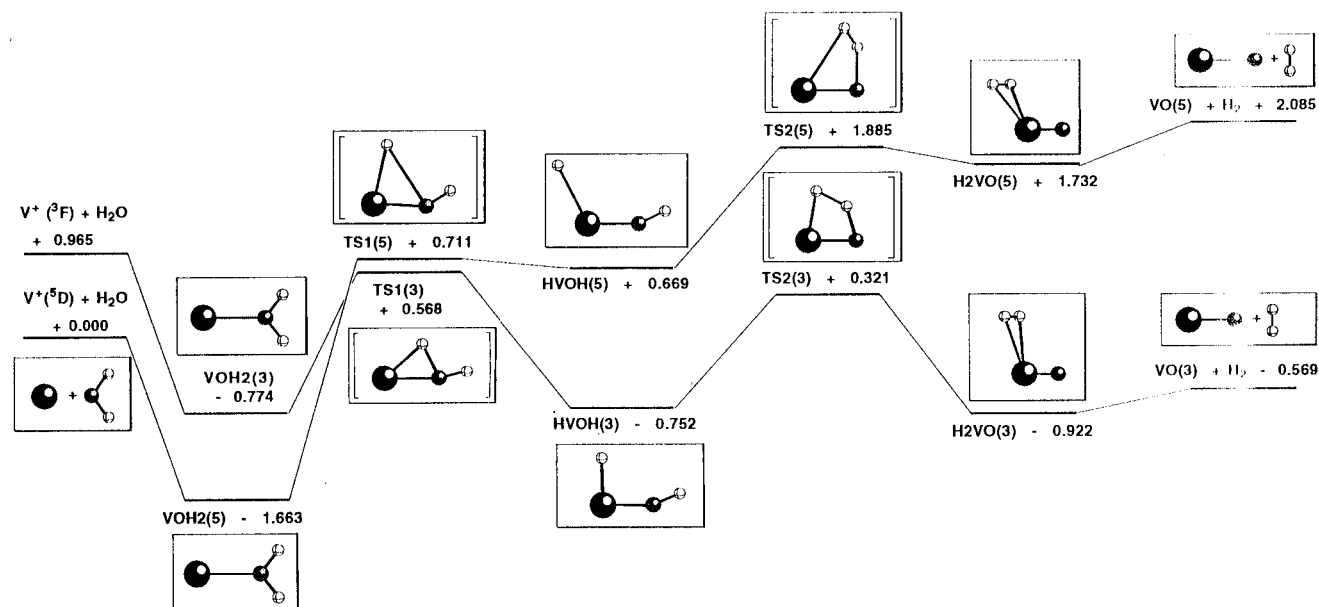


Figure 7. B3LYP/DZVP potential energy surface following the $\text{V}^+ + \text{OH}_2 \rightarrow \text{VO}^+ + \text{H}_2$ reaction path. Energies given are in electronvolts and are relative to the separated ground-state reactants, $\text{V}^+(\text{5D}) + \text{OH}_2$.

states at the B3LYP/DZVP level of theory for Sc and V, respectively. That the different spin structures are located in the same column should not be taken to mean that they are connected by simple vertical excitation. The geometrical parameters are significantly different, as can be seen in Figures 2–5.

On both low-spin surfaces, the first step is the formation of the ion–molecule complex. Then, through TS1 , one hydrogen atom is passed from oxygen to the metal, leading to the HM^+OH molecule, the intermediate whose existence was surmised by experimentalists. Here we observe one of the important differences between V and Sc and Ti. That is, on the V triplet-state surface, the TS1 transition state lies above the energy of the $\text{V}^+(\text{5D}) + \text{H}_2\text{O}$ reactants by 0.568 eV, while the singlet TS1 on the Sc surface lies energetically below the $\text{Sc}^+(\text{3D}) + \text{H}_2\text{O}$ reactants by 0.364 eV. The corresponding value

for the Ti doublet surface is +0.056 eV, that is, almost isoenergetic with the separated reactants.

Here we have a possible explanation for the observed experimental behavior of the ground-state metal cations when reacting with water. Both $\text{Sc}^+(\text{3D})$ and $\text{Ti}^+(\text{4F})$ are seen to exhibit at least some spin-forbidden crossing, leading to low-spin products.⁶ $\text{V}^+(\text{5D})$, however, does not make that crossing.⁵ The low- and high-spin surfaces must cross between the $\text{M}(\text{OH}_2)^+$ and HM^+OH moieties since the relative positions are switched. In the case of Sc and Ti, that crossing of surfaces occurs at an energy below that of the high-spin reactants, whereas in the case of V, the crossing occurs at an energy above that of the reactants according to our calculations. Also, it is clear that the reactivity through this pathway should decrease from Sc to V as the initial activation energy needed to go through TS1 increases. Of course, some caution must be taken with these

numbers because dynamical factors, too, would play a role in the evolution of the reaction.

As noted earlier, the 5F state of V^+ does demonstrate some surface crossing. The main differences between the 5D and 5F states of V^+ are the occupation scheme (d^4 for 5D vs sd^3 for 5F) and the relative energy. Which, then is the cause of the difference in reactivity?

If the reaction path we propose here (and that suggested by others^{5,6}) is the true path of the reaction, then the occupation scheme should not cause a difference by arguments of symmetry. Both the 5D and 5F initial states transform smoothly to the same 5A_1 $V(OH_2)^+$ ion–molecule complex. Considering this, we investigated the energy of the triplet TS1 at the B3LYP/TZVP+G(3df,2p) level of theory and found it to lie 0.473 eV above the separated $V(^5D) + H_2O$ reactants. The 5F state of V^+ at that same level of theory lies 0.557 eV above the 5D state, and thus our mystery is solved, or at least the energetic argument is strengthened. The reactants starting with V^+ in the 5F state do have enough energy to reach the point where the surfaces cross and, therefore, $VO(^3\Sigma)$ is produced (though inefficiently), whereas the reactants in their ground state do not have enough energy to reach the point where the crossing is made.

It should also be pointed out that the open-shell singlet $Sc(OH_2)^+$ species is converted to the closed-shell singlet HSc^+OH isomer in the process of H transfer. The passing of the H atom occurs through this near- C_s structure, which mixes the two singly occupied orbitals and falls to the lower-energy (at this point) electronic structure of the closed-shell singlet.

The HSc^+OH singlet state is much more stable than the $Sc(OH_2)^+$ singlet species (1.492 eV), while the HTi^+OH doublet state is more stable than the $Ti(OH_2)^+$ doublet species by 0.626 eV. In contrast, on the triplet surface of V, we found that the triplet $HVOH^+$ isomer is actually 0.22 eV *less* stable than the corresponding $V(OH_2)^+$ triplet species.

The second hydrogen transfer from oxygen to the metal takes place through TS2. Again this transition state lies lower in energy than the reactants for Sc and Ti low-spin structures, but not for the V triplet transition state. This transition state leads to the final intermediate found on the reaction path: the $(H_2)MO^+$ ion–molecule complex. In the case of $M = Sc$, this complex is bound by 0.270 eV, while it is bound by 0.375 eV in the case of Ti and 0.353 eV for V. It should be remembered that the bonding of this complex is very different for Sc due to the lack of singly occupied d orbitals (see Stationary Points section). From this intermediate, the loss of H_2 proceeds without transition state to the observed major products, low-spin MO^+ and H_2 .

The first step on the high-spin surface can also be formation of the ion–molecule complex. However, following the reaction from that point is significantly more complicated than was the case for the low-spin surfaces. Despite numerous varied strategies for finding a transition state between this complex and the HSc^+OH molecule, none was found, as happened in the Ti quartet surface. But this was not the case for the quintet surface for V: a quintet TS1 has been found in this surface corresponding to the migration of one hydrogen from oxygen to vanadium, and this high-spin transition state is less stable than the corresponding triplet TS1 by 0.143 eV.

Once the high-spin HM^+OH intermediate is formed, another intermediate, $(H_2)MO^+$, can be realized by passing through another high-lying H transfer transition state, TS2. This TS2 is

much less stable than the corresponding low-spin TS2. From that isomer, the loss of an H_2 molecule gives one of the scarcely observed reaction products, high-spin MO^+ . The high relative energy of this product agrees well with the fact that MO^+ in this spin state is a rarely observed reaction product.

Equilibrium geometry parameters for the various reaction products are given in Figures 8 and 9 (Supporting Information).

4. Conclusions

The reactions of Sc^+ and V^+ with water have been investigated in detail, completing this study of the reactivity of the early first-row transition metals. Both the low- and high-spin potential energy surfaces have been characterized at the B3LYP/DZVP level of theory. Energy differences between key low- and high-spin species and total reaction energies for the experimentally observed products have been predicted at even higher levels of theory, including B3LYP/TZVP+G(3df,2p) and CCSD(T)/TZVP+G(3df,2p). From these data, the following conclusions are drawn:

(1) The only exothermic products of the $M^+ + H_2O$ reaction are the ones corresponding to formation of $MO^+ + H_2$ at their low-spin ground state. The exothermicity of these reactions decreases from Sc to V.

(2) The HM^+OH intermediate hypothesized by the experimentalists is a well-defined minimum on each potential energy surface. HSc^+OH and HTi^+OH lie lower than the corresponding $M(OH_2)^+$ ion–molecule complex, while the contrary is true for V.

(3) The low- and high-spin potential energy surfaces cross between this aforementioned intermediate and the $M(OH_2)^+$ ion–molecule complex. In the cases of Sc and Ti, the crossing of surfaces occurs at an energy below that of the high-spin reactants, whereas in the case of V, the crossing occurs at an energy *above* that of the ground-state reactants. It has been shown that such a crossing is possible from the $V(^5F)$ excited state due to its elevated energy according to the level of theory applied.

(4) The H_2 elimination process passes from the HM^+OH intermediate through a four-centered transition state to an ion–molecule intermediate $(H_2)MO^+$, from which intermediate H_2 is eliminated without transition state. In the case of $(H_2)ScO^+$, this ion–molecule complex is planar, whereas the $(H_2)TiO^+$ and $(H_2)VO^+$ complexes are minima when the (H_2) unit is coordinated perpendicular to the MO^+ unit. This is due to the fact that there are no occupied d orbitals in ScO^+ , which could exemplify $d \rightarrow \sigma_{H-H}^*$ donation.

Acknowledgment. A.I. and J.E.F. thank the Basque Government (Eusko Jaurlaritza) for a grant. Financial support from the Spanish DGICYT Grant No. PB96/1524 and from the Provincial Government of Gipuzkoa (Gipuzkoako Foru Aldundia) is gratefully acknowledged.

Supporting Information Available: Figures 8 and 9, showing equilibrium geometry parameters for the various $Sc^+ + OH_2$ and $V^+ + OH_2$ reaction products at the B3LYP/DZVP level of theory, along with parameters predicted at the B3LYP/TZVP+G(3df,2p) level of theory (2 pages, print/PDF). See any current masthead page for ordering information and Web access instructions.